Pergamon

Int. J. Solids Structures Vol. 35, Nos. 1–2, pp. 107–127, 1998

0020–7683/98 $19.00 + .00

PII: S0020–7683(97)00060–7

ON THE ANALYSIS OF CROSS-PLY LAMINATES WITH MICRO-CRACKS AND INELASTIC DEFORMATION

ZHANJUN GAO†
Department of Mechanical & Aeronautical Engineering, Clarkson University, Potsdam, NY 13699, U.S.A.

and

JOSEPH R. ZUIKER‡
Wright Laboratory Materials Directorate, WL/MLLN Bldg 655, 2230 Tenth Street, Suite 1, Wright-Patterson AFB, OH 45433-7817, U.S.A.

(*Received* 23 *April* 1996, *in revised form* 30 *September* 1996)

Abstract—For cross-ply laminates micro-matrix cracks in the 90° plies and inelastic deformation in the 0° and 90° plies are two major forms of damage which affect the long-term durability of the materials. It is crucial to develop a mechanics based approach to incorporate both micro-cracks and inelastic deformation of the composite materials based on the response of the 0° and 90° plies in order to accurately predict the response of the materials in service environments and to assist in optimizing the materials system for best performance. However, such a task leads to severe mathematical difficulties, primarily due to the zero traction conditions on the crack surfaces, the complicated constitutive relations governing the inelastic deformation and the interaction between the cracks and the inelastic deformation. In this paper, a general framework for the analysis of cross-ply laminates with micro-matric cracks and inelastic deformation is proposed. For this purpose admissible stress fields are constructed which satisfy equilibrium and all boundary and interface conditions. The principle of minimum complementary energy is utilized to derive a differential equation for the stress function from which the stress field of the composite can be derived. The inhomogeneous terms of the differential equation involve the inelastic strains which are loading history dependent. The Green's function of the differential equation is then obtained. Using the Green's function and a constitutive equation, two-dimensional stress and strain states in the composite at any time are represented by an integral of the Green's function and the inelastic strains accumulated up to that time. This new analysis takes into consideration the microcrack–microcrack interaction, as well as the interaction between the microcracks and the inelastic deformation, and provides a point-wise variation of the stress field instead of average stress field as most of the analytical approaches yield.

The interactions of matrix cracks and creep deformation of an eight-harness satin weave (8HSW) Nextel 610/Aluminosilicate ceramic matrix composite is studied using the proposed model. The predicted creep strain of the composite shows good correlation with experimental data at different levels of temperature and stress conditions. The distribution of stresses and strains provides important information on the response of the composite. © 1997 Elsevier Science Ltd.

INTRODUCTION

Under static or cyclic loading, composite laminates may develop intralaminar cracks which extend along the fibers, transverse to the plies as shown in Fig. 1. One direct effect of such cracks on laminate properties is the reduction of stiffness. There has been much interest in this problem in recent years. Among others, Highsmith and Reifsnider (1982) treated the problem in terms of a shear-lag analysis. Laws *et al.* (1983) employed a self-consistent model to assess the stiffness reduction of a cracked lamina in a laminate. Talreja (1985) proposed a continuous damage mechanics theory to represent the cracks with damage parameters. A variational approach was proposed by Hashin (1985) which yields a stress

† Present address: Eastman Kodak Company, 1669 Lake Avenue, Rochester, NY 14652-4333, U.S.A.
‡ Present address: GE Corporate Research and Development, P.O. Box 8, Schenectady, NY 12301, U.S.A.

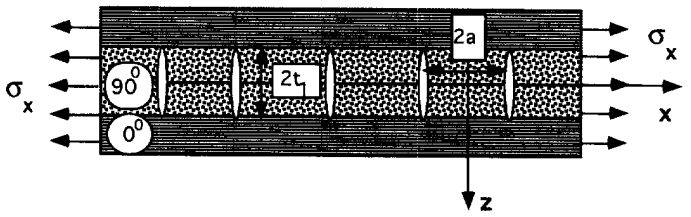

Fig. 1. A schematic representation of a cross-ply laminate with matrix cracks in the 90° plies. Here $2a$ is the distance of two cracks between which the stresses and strains are to be solved. It should be noted at the crack spacing need not be uniform.

field more accurate than the simple shear-lag analysis. Furthermore, Narin (1989) has shown that a better analytical result by variational approach cannot be obtained. One of the advantages of the variational solution is that it accurately includes transverse stresses and therefore distinguishes between $[0_m/90_n]_s$ and $[90_n/0_m]_s$ laminates. The shear-lag analyses (Parvizi *et al.* 1978; Bailey *et al.* 1979; Highsmith and Reifsnider, 1982; Flaggs, 1985) do not distinguish between $[0_m/90_n]_s$ and $[90_n/0_m]_s$ laminates. McCartney (1992) has developed two analytical methods for cross-ply laminate containing transverse cracks under the framework of the 2-D and 3-D elasticity. It should be noted that inelastic deformation of the matrix and fiber materials is not considered in the above analyses.

Inelastic deformation such as creep deformation is another important phenomenon which has direct impact on the performance of the composite materials, especially for structures intended for high temperature applications such as advanced turbine engines. During elastic deformation of the composite materials, the constituent phases are homogeneous and their properties are known constants. This simplifies modeling to a great extent because the local stress and strain fields, as well as their averages are linearly related by the constant stiffness and compliance tensors. Overall properties can be evaluated from the phase field averages that can be found from solutions of certain inclusion problems in a representative volume of the aggregate. When at least one of the phases deforms inelastically, its local properties depend on the deformation history, and the phase is no longer homogeneous. Numerical analysis becomes nonlinear and must generally be solved in an incremental manner which can significantly increase the computation effort. A variety of techniques have been invoked to deal with these issues. Most computationally efficient is to treat the inelastic composite as an effective homogeneous medium which follows an anisotropic inelastic constitutive law (e.g., Krempl and Hong, 1989). An alternative is to generate estimates of the stress and strain states in both the fiber and matrix. The simplest of these circumvent the difficulty of estimating stress, strain, and effective property distributions throughout the inelastic phase by assuming that the local fields are uniform (Dvorak and Bahei-El-Din, 1982). Other models approximate in various ways the actual nonuniform fields (Aboudi, 1991; Coker *et al.*, 1993; Kroupa *et al.*, 1996), while at least one such approach also provides upper and lower bounds on certain instantaneous stiffness and compliance coefficients (Teply and Dvorak, 1988). An overview of such techniques is given by Dvorak (1991).

It is crucial to develop a mechanics based approach to incorporate both microstructural damage (crack in the present case) and inelastic deformation of composite materials based on the response of the 0° and 90° plies in order to accurately predict the response of the material in service environments and to assist in optimizing the materials system for the best performance. However, such a task leads to severe mathematical difficulties, primarily due to the zero traction conditions on the crack surfaces, the complicated constitutive relations governing the inelastic deformation and the interaction between the cracks and inelastic deformation. In this paper, a variational approach is proposed to establish a general framework for analyzing composites with both matrix cracks and inelastic deformation. The response of an eight-harness satin weave (8HSW) Nextel 610/Aluminosilicate ceramic matrix composite is analyzed using the proposed model. An approximation to the eight-harness satin weave (8HSW) is made, following the mosaic model (Ishikawa and Chou, 1983) which treats woven composites as cross-ply laminates. Such a treatment provides a

good representation of stresses and strains away from the region where the fibers cross, and has been used previously by Zuiker (1996).

VARIATION FORMULATION FOR COMPOSITES WITH MATRIX CRACKS AND INELASTIC DEFORMATION

An admissible stress field for cross-ply laminate under tension with cracks in 90° plies, Fig. 1, is constructed by using the approach suggested by Hasin (1985) for a cracked cross-ply with no inelastic deformation. It is assumed that σ_{xx} is a function of x only, and $\sigma_{yz} = \sigma_{xy} = 0$. The ramifications of the assumption are discussed in Appendix A. For now is suffices to note that all shear-lag analyses make the same assumption along with a host of additional assumptions (Narin, 1989). The systematic integration of the equations of equilibrium, taking into account traction continuity and boundary conditions defines an admissible stress field in terms of an unknown function, $\phi(x)$, as follows

$$\sigma_{11}^{(90^\circ)} = \sigma_{xx}^{(90^\circ)} = \sigma_{xx0}^{(90^\circ)}[1-\phi(x)]$$

$$\sigma_{11}^{(0^\circ)} = \sigma_{xx}^{(0^\circ)} = \sigma_{xx0}^{(0^\circ)} + \frac{1}{\lambda}\sigma_{xx0}^{(90^\circ)}\phi(x)$$

$$\sigma_{13}^{(90^\circ)} = \sigma_{xz}^{(90^\circ)} = \sigma_{xx0}^{(90^\circ)}\phi'(x)z$$

$$\sigma_{13}^{(0^\circ)} = \sigma_{xz}^{(0^\circ)} = \frac{1}{\lambda}\sigma_{xx0}^{(90^\circ)}\phi'(x)(h-z),$$

$$\sigma_{22}^{(90^\circ)} = \sigma_{yy}^{(90^\circ)} = \sigma_{yy0}^{(90^\circ)}$$

$$\sigma_{22}^{(0^\circ)} = \sigma_{yy}^{(0^\circ)} = \sigma_{yy0}^{(0^\circ)}$$

$$\sigma_{33}^{(90^\circ)} = \sigma_{zz}^{(90^\circ)} = \tfrac{1}{2}\sigma_{xx0}^{(90^\circ)}\phi''(x)[ht_1 - z^2]$$

$$\sigma_{33}^{(0^\circ)} = \sigma_{zz}^{(0^\circ)} = \frac{1}{2\lambda}\sigma_{xx0}^{(90^\circ)}\phi''(x)[h-z]^2$$

$$h = t_2 + t_1 \quad \lambda = t_2/t_1 \tag{1}$$

where superscripts 0° and 90° represent the 0° and 90° plies, respectively, prime indicates derivative with respect to x, and t_1 is the thickness of one 90° ply, and t_2 is the thickness of one 0° ply. The stresses in undamaged (no cracks or inelastic deformation) and damaged laminates are denoted by σ_0 and σ. For instance, $\sigma_{xx0}^{(90^\circ)}$ and $\sigma_{xx}^{(90^\circ)}$ denote the x direction normal stresses of the 90° plies in the undamaged and damaged laminates, respectively. The stress free conditions, $\sigma_{xx}^{(90^\circ)} = \sigma_{xz}^{(90^\circ)} = 0$, on the crack surfaces, $x = \pm a$, lead to the boundary conditions for function, $\phi(x)$,

$$\phi(\pm a) = 1, \quad \frac{\mathrm{d}\phi}{\mathrm{d}x}(\pm a) = 0 \tag{2}$$

where a is the half of the distance between the two cracks being analyzed as shown in Fig. 1. Equations (1) and (2) represent the stress field between two cracks at $x = a$ and $x = -a$. Between cracks located away from the origin, the stress fields can still be defined in the form of eqn (1), with the boundary condition revised to

$$\phi(\text{crack faces}) = 1, \quad \frac{\mathrm{d}\phi}{\mathrm{d}x}(\text{crack faces}) = 0. \tag{2'}$$

Therefore, the matrix crack spacing need not be uniform.

The complementary energy of the composite is given by

$$\Gamma = \frac{1}{2}\iiint_V S_{ijkl}\sigma_{ij}\sigma_{kl}\,dV + \iiint_V \sigma_{ij}\alpha_{ij}\,\Delta T\,dV + \Gamma^{in} \tag{3}$$

where S_{ijkl}, α_{ij}, ΔT are the compliance tensor, thermal expansion coefficient tensor and the temperature difference between the current temperature and the stress free temperature, respectively; Γ^{in} represents the contribution of the inelastic strain to the complementary energy of the system, which will be discussed in some detail later.

The first two terms in Γ for the region between two micro-cracks; i.e., for the region $-a < x < a$ and $-h < z < h$ are evaluated by substituting the stress expressions in eqn (1) into eqn (3). Therefore,

$$\begin{aligned}\Gamma = \Gamma^0 &+ (\sigma_{xx0}^{(90^\circ)})^2 \int_{-a}^{a} dx \int_0^{t_1} dz \left[-\frac{2\phi}{E_T} - \frac{v_T(ht_1 - z^2)\phi''}{E_T} \right. \\ &+ \frac{\phi^2}{E_T} + \frac{v_T(ht_1 - z^2)\phi\phi''}{E_T} + \frac{(ht_1 - z^2)^2\phi''\phi''}{4E_T} + \frac{z^2\phi'\phi'}{G_T} \\ &\left. -2\alpha_T\Delta T\phi + \alpha_T\Delta T(ht_1 - z^2)\phi'' \right] \\ &+ (\sigma_{xx0}^{(90^\circ)})^2 \int_{-a}^{a} dx \int_{t_1}^{h} dz \left[\frac{2\phi}{\lambda E_A} - \frac{v_A(h-z)^2\phi''}{\lambda E_A} \right. \\ &+ \frac{\phi^2}{\lambda^2 E_A} - \frac{v_A(h-z)^2\phi\phi''}{\lambda^2 E_T} + \frac{(h-z)^4\phi''\phi''}{4\lambda^2 E_T} + \frac{(h-z)^2\phi'\phi'}{\lambda^2 G_A} \\ &\left. + \frac{2\alpha_A\Delta T\phi}{\lambda} + \frac{\alpha_T\Delta T(h-z)^2\phi''}{\lambda} \right] + \Gamma^{in}\end{aligned}$$

where

$$\Gamma^0 = \int_{-a}^{a} dx \int_0^{t_1} dz \left[\frac{\sigma_{xx0}^{(90^\circ)}}{E_T} + 2\alpha_T\Delta T \right] \sigma_{xx0}^{(90^\circ)} + \int_{-a}^{a} dx \int_{t_1}^{h} dz \left[\frac{\sigma_{xx0}^{(0^\circ)}}{E_A} + 2\alpha_A\Delta T \right] \sigma_{xx0}^{(0^\circ)}$$

is the complementary energy of the laminate without any damage or inelastic deformation. Let $\xi = x/t_1$ and the expression for Γ can be simplified as

$$\begin{aligned}\Gamma = \Gamma^0 + (\sigma_{xx0}^{(90^\circ)})^2 (t_1)^2 \int_{-\rho}^{\rho} &[C_1\phi^2 + C_2\phi\phi'' + C_3(\phi'')^2 + C_4(\phi')^2 \\ &- 2(\alpha_T - \alpha_A)\Delta T\phi + C_5\phi''] \, d\xi + \Gamma^{in}\end{aligned} \tag{4}$$

where $\rho = a/t_1$, E_A, E_T, G_A, G_T, v_A, v_T, α_A, α_T, are the effective axial and transverse Young's moduli, shear moduli, Poisson's ratios, and thermal expansion coefficients of the unidirectional composite, respectively, and

$$C_1 = \frac{hE_0}{t_2 E_A E_T} \quad C_2 = \frac{v_T}{E_T}\left(\lambda + \frac{2}{3}\right) - \frac{\lambda}{3}\frac{v_A}{E_A}$$

$$C_3 = \frac{\lambda + 1}{60E_T}(3\lambda^2 + 12\lambda + 8) \quad C_4 = \frac{1}{3}\left(\frac{1}{G_T} + \frac{\lambda}{G_A}\right)$$

$$C_5 = \left(\alpha_T \Delta T - \frac{\nu_T}{E_o}\sigma_{\text{applied}}\right)\left(\lambda + \frac{2}{3}\right) + \left(\alpha_T \Delta T - \frac{\nu_A}{E_0}\sigma_{\text{applied}}\right)\frac{\lambda^2}{3}.$$

The applied load on the composite is shown in terms of stress as σ_{applied} in the above expression, and E_0 is the Young's modulus of the undamaged cross-ply laminate in the 0° ply fiber direction. The derivation of eqn (4) is similar to that given by Narin (1989) for a cross-ply laminate without inelastic deformation.

The first order variation of the functional Γ, $\delta\Gamma$, is found using eqn (4)

$$\delta\Gamma = (\sigma_{xx0}^{(90^\circ)})^2 (t_1)^2 \int_{-\rho}^{\rho} [2C_1\phi\,\delta\phi + C_2(\phi\,\delta\phi'' + \delta\phi\phi'') + 2C_3\phi''\,\delta\phi'' + 2C_4\phi'\,\delta\phi' - 2(\alpha_T - \alpha_A)\,\Delta T\,\delta\phi + C_5\,\delta\phi'']\,\mathrm{d}\xi + \delta\Gamma^{in}.$$

The above equation is simplified through integration by parts and use of the boundary condition in eqn (2)

$$\delta\Gamma = 2C_3(\sigma_{xx0}^{(90^\circ)})^2 (t_1)^2 \int_{-\rho}^{\rho} \left[\frac{\mathrm{d}^4\phi(\xi)}{\mathrm{d}\xi^4} + p\frac{\mathrm{d}^2\phi(\xi)}{\mathrm{d}\xi^2} + q\phi(\xi) - \frac{(\alpha_T - \alpha_A)\,\Delta T}{C_3}\right]\delta\phi(\xi)\,\mathrm{d}\xi + \delta\Gamma^{in}$$

where $p = (C_2 - C_4)/C_3$ and $q = C_1/C_3$.

The contribution of the inelastic strain, ε_{ij}^{in}, to the variation of the total complimentary energy is given as

$$\begin{aligned}
\delta\Gamma^{in} &= \iiint_V \varepsilon_{ij}^{in}\,\delta\sigma_{ij}\,\mathrm{d}V \\
&= \int_{-a}^{a}\mathrm{d}x\int_0^{t_1}\mathrm{d}z\{\varepsilon_{11}^{in(90^\circ)}\,\delta\sigma_{11}^{(90^\circ)} + \varepsilon_{33}^{in(90^\circ)}\,\delta\sigma_{33}^{(90^\circ)} + 2\varepsilon_{13}^{in(90^\circ)}\,\delta\sigma_{13}^{(90^\circ)}\} \\
&\quad + \int_{-a}^{a}\mathrm{d}x\int_{t_1}^{h}\mathrm{d}z\{\varepsilon_{11}^{in(0^\circ)}\,\delta\sigma_{11}^{(0^\circ)} + \varepsilon_{33}^{in(0^\circ)}\,\delta\sigma_{33}^{(0^\circ)} + 2\varepsilon_{13}^{in(0^\circ)}\,\delta\sigma_{13}^{(0^\circ)}\} \\
&= \sigma_{xx0}^{(90^\circ)}\int_{-a}^{a}\mathrm{d}x\int_0^{t_1}\mathrm{d}z\{\varepsilon_{11}^{in(90^\circ)}\,\delta[-\phi] + \varepsilon_{33}^{in(90^\circ)}\,\delta\left[\frac{1}{2}\phi''(x)(ht_1 - z^2)\right] \\
&\quad + 2\varepsilon_{13}^{in(90^\circ)}\,\delta[\phi''(x)z]\} \\
&\quad + \sigma_{xx0}^{(90^\circ)}\int_{-a}^{a}\mathrm{d}x\int_{t_1}^{h}\mathrm{d}z\left\{\varepsilon_{11}^{in(0^\circ)}\,\delta\left[\frac{\phi}{\lambda}\right] + \varepsilon_{33}^{in(0^\circ)}\,\delta\left[\frac{1}{2\lambda}\phi''(x)(h-z)^2\right]\right. \\
&\quad \left. + 2\varepsilon_{13}^{in(0^\circ)}\left[\frac{1}{\lambda}\phi'(x)(h-z)\right]\right\}.
\end{aligned}$$

Let $\xi = x/t_1$ and $\omega = z/t_1$, we have

$$\begin{aligned}
\delta\Gamma^{in} &= (t_1)^2\sigma_{xx0}^{(90^\circ)}\int_{-\rho}^{\rho}\{A_1(\xi)\,\delta\phi(\xi) + A_2(\xi)\,\delta\phi''(\xi) + A_3(\xi)\,\delta\phi'(\xi)\}\,\mathrm{d}\xi \\
&\quad + (t_1)^2\sigma_{xx0}^{(90^\circ)}\int_{-\rho}^{\rho}\{B_1(\xi)\,\delta\phi(\xi) + B_2(\xi)\,\delta\phi''(\xi) + B_3(\xi)\,\delta\phi'(\xi)\}\,\mathrm{d}\xi
\end{aligned}$$

$$= (t_1)^2\sigma_{xx0}^{(90^\circ)}\int_{-\rho}^{\rho}\left\{A_1(\xi)+\frac{d^2A_2(\xi)}{d\xi^2}-\frac{dA_3(\xi)}{d\xi}\right\}\delta\phi(\xi)\,d\xi$$

$$+(t_1)^2\sigma_{xx0}^{(90^\circ)}\int_{-\rho}^{\rho}\left\{B_1(\xi)+\frac{d^2B_2(\xi)}{d\xi^2}-\frac{dB_3(\xi)}{d\xi}\right\}\delta\phi(\xi)\,d\xi \tag{6}$$

where

$$A_1(\xi) = -\int_0^1 \varepsilon_{11}^{in(90^\circ)}\,d\omega \tag{7}$$

$$A_2(\xi) = \int_0^1 \frac{1}{2}[h/t_1-\omega^2]\varepsilon_{33}^{in(90^\circ)}\,d\omega \tag{8}$$

$$A_3(\xi) = 2\int_0^1 \varepsilon_{13}^{in(90^\circ)}\omega\,d\omega \tag{9}$$

$$B_1(\xi) = \frac{1}{\lambda}\int_1^{h/t_1} \varepsilon_{11}^{in(0^\circ)}\,d\omega \tag{10}$$

$$B_2(\xi) = \frac{1}{2\lambda}\int_1^{h/t_1} (h/t_1-\omega)^2\varepsilon_{33}^{in(0^\circ)}\,d\omega \tag{11}$$

$$B_3(\xi) = 2\frac{1}{\lambda}\int_1^{h/t_1} (h/t_1-\omega)\varepsilon_{13}^{in(0^\circ)}\,d\omega. \tag{12}$$

Substituting eqn (6) into eqn (5) and using the condition $\delta\Gamma = 0$, one obtains

$$\delta\Gamma = 2C_3(\sigma_{xx0}^{(90^\circ)})^2(t_1)^2\int_{-\rho}^{\rho}\left\{\frac{d^4\phi(\xi)}{d\xi^4}+p\frac{d^2\phi(\xi)}{d\xi^2}+q\phi(\xi)-\frac{(\alpha_T-\alpha_A)\,\Delta T}{C_3}\right.$$

$$\left.+\frac{1}{2C_3\sigma_{xx0}^{(90^\circ)}}\left[A_1(\xi)+\frac{d^2A_2(\xi)}{d\xi^2}-\frac{dA_3(\xi)}{d\xi}+B_1(\xi)+\frac{d^2B_2(\xi)}{d\xi^2}-\frac{dB_3(\xi)}{d\xi}\right]\right\}\delta\phi(\xi)\,d\xi$$

which leads to the governing equation for the function $\phi(\xi)$

$$\frac{d^4\phi(\xi)}{d\xi^4}+p\frac{d^2\phi(\xi)}{d\xi^2}+q\phi(\xi) = F(\xi) \tag{13}$$

where

$$F(\xi) = \frac{(\alpha_T-\alpha_A)\,\Delta T}{C_3}-\frac{1}{2C_3\sigma_{xx0}^{(90^\circ)}}\left\{A_1(\xi)+\frac{d^2A_2(\xi)}{d\xi^2}-\frac{dA_3(\xi)}{d\xi}+B_1(\xi)+\frac{d^2B_2(\xi)}{d\xi^2}-\frac{dB_3(\xi)}{d\xi}\right\}$$

is related to the stress function, $\phi(\xi)$, and ξ through the inelastic strains $\varepsilon_{ij}^{in(90^\circ)}$ and $\varepsilon_{ij}^{in(0^\circ)}$. The boundary conditions for eqn (13) is, from eqn (2),

$$\phi(\xi)\,|_{\xi=\pm\rho} = 1, \quad \left.\frac{d\phi(\xi)}{d\xi}\right|_{\xi=\pm\rho} = 0. \tag{14}$$

CONSTITUTIVE EQUATIONS

The inhomogeneous term, $F(\xi)$, in eqn (13) is related to the inelastic strains of the laminate which are loading history dependent. This section deals with the constitutive relationships which describe such strains using the response of the 0° and 90° plies. Without losing generality, creep deformation is used here to demonstrate the proposed model. Any other constitutive model can be used as well.

A one dimensional creep law is gven by Dorn's law (Mukherjee *et al.*, 1969)

$$\dot{\varepsilon}^c = A\left\{\frac{|\sigma|}{G}\right\}^n \frac{Gb}{kT} D_0 \exp\left\{-\frac{Q}{RT}\right\} \tag{15}$$

where $\dot{\varepsilon}^c$ and σ are the creep rate and stress of the material, A and n are constants that can be determined experimentally, G is the shear modulus, b is the Burger's vector, k is Boltzmann's constant, D_0 is a pre-exponential constant, Q is the activation energy for self-diffusion, and T is the temperature.

For two-dimensional and three-dimensional problems, the Prandtl–Reuss relations can be used for computing the creep increments. Thus the equivalent creep strain rate is written as

$$\dot{\varepsilon}^{c,eff} = A\left\{\frac{\sigma^{eff}}{G}\right\}^n \frac{Gb}{kT} D_0 \exp\left\{-\frac{Q}{RT}\right\} \tag{16}$$

where σ^{eff}, is the von Mises' effective stress which is defined as

$$\sigma^{eff} = \sqrt{\left(\tfrac{3}{2}\sigma^*_{ij}\sigma^*_{ij}\right)} \tag{17}$$

and σ^*_{ij} is the deviatoric stress tensor. Then, using the Prandtl–Reuss flow law, the creep strain rate tensor is defined as

$$\dot{\varepsilon}^c_{ij} = \frac{3}{2}\frac{\dot{\varepsilon}^{c,eff}}{\sigma^{eff}}\sigma^*_{ij}. \tag{18}$$

Note that

$$\dot{\varepsilon}^{c,eff} = \sqrt{\left(\tfrac{2}{3}\dot{\varepsilon}^c_{ij}\dot{\varepsilon}^c_{ij}\right)}. \tag{19}$$

Equations (16) and (18) can be written in incremental forms

$$\Delta\varepsilon^{c,eff} = A\left\{\frac{\sigma^{eff}}{G}\right\}^n \frac{Gb}{kT} D_0 \exp\left\{-\frac{Q}{RT}\right\}\Delta t \tag{21}$$

$$\Delta\varepsilon^c_{ij} = \frac{3}{2}\frac{\Delta\varepsilon^{c,eff}}{\sigma^{eff}}\sigma^*_{ij} = \frac{3}{2}A\left(\frac{1}{G}\right)^n \frac{Gb}{kT} D_0 \exp\left\{-\frac{Q}{RT}\right\}(\sigma^{eff})^{(n-1)}\sigma^*_{ij}\Delta t. \tag{22}$$

Therefore, the total creep strain at the instant, $t+\Delta t$, is

$$\varepsilon^c_{ij} = \varepsilon^{co}_{ij} + \Delta\varepsilon^c_{ij} = \varepsilon^{co}_{ij} + (\sigma^{eff})^{(n-1)}\sigma^*_{ij} w\,\Delta t \tag{23}$$

where ε_{ij}^{co} is the creep strain at time t, σ^{eff} and σ_{ij}^{*} are the effective stress and deviatoric stress at time $t+\Delta t$; and w is independent of stress and is defined as

$$w = \frac{3}{2} A \left(\frac{1}{G}\right)^{n} \frac{Gb}{kT} D_0 \exp\left\{-\frac{Q}{RT}\right\} \tag{24}$$

where T is the temperature at time $t+\Delta t$.

The constitutive law in eqns (16)–(23) are for isotropic materials. To apply them to a transversely isotropic lamina, different values of exponents are used

$$\varepsilon_{ij}^{c(90^\circ)} = \varepsilon_{ij}^{co(90^\circ)} + \Delta\varepsilon_{ij}^{c(90^\circ)} = \varepsilon_{ij}^{co(90^\circ)} + (\sigma^{eff})^{(n_m-1)} \sigma_{ij}^{*} w_m \Delta t \tag{25}$$

$$\varepsilon_{ij}^{c(0^\circ)} = \varepsilon_{ij}^{co(0^\circ)} + \Delta\varepsilon_{ij}^{c(0^\circ)} = \varepsilon_{ij}^{co(0^\circ)} + (\sigma^{eff})^{(n_f-1)} \sigma_{ij}^{*} w_f \Delta t \tag{26}$$

where n_m and w_m are the parameters for creep deformation in the 90° plies obtained from a creep test of a unidirectional lamina with loading transverse to the fiber direction. Similarly, n_f and w_f are the parameters for the 0° plies obtained from a creep test of a unidirectional lamina with loading along the fiber direction. It should be noted that this formulation in its current form produces isotropic creep response in each ply. Although this is not an accurate characterization for the unidirectional ply under arbitrary loading, it is sufficient for the cases considered here wherein the laminate is loaded only in the 0° fiber direction. The effect of the longitudinal stress in the 90° plies will not be accurately accounted for in this approximation. However, for the case of 0° loading, that stress is small in comparison to those in the loading direction and is expected to have negligible effect on the overall composite response. An alternative approach is, of course, to introduce an anisotropic creep formulation.

When creep is the only source of inelastic deformation, $\varepsilon_{ij}^{in(90^\circ)}$ and $\varepsilon_{ij}^{in(0^\circ)}$ in eqns (7)–(12) are replaced by the creep strains $\varepsilon_{ij}^{c(90^\circ)}$ and $\varepsilon_{ij}^{c(0^\circ)}$, respectively. The creep strains are related to stresses in each ply which are expressed in terms of the stress function, $\phi(\xi)$, as well as ξ and ω. The expressions of stresses are obtained from eqn (1) and the relationships $\xi = x/t_1$ and $\omega = z/t_1$ as

$$\begin{aligned}
\sigma_{11}^{(90^\circ)} &= \sigma_{xx0}^{(90^\circ)}[1-\phi(\xi)] \\
\sigma_{11}^{(0^\circ)} &= \sigma_{xx0}^{(0^\circ)} + \frac{1}{\lambda}\sigma_{xx0}^{(90^\circ)}\phi(\xi) \\
\sigma_{13}^{(90^\circ)} &= \sigma_{xx0}^{(90^\circ)}\omega\frac{\mathrm{d}\phi(\xi)}{\mathrm{d}\xi} \\
\sigma_{13}^{(0^\circ)} &= \frac{1}{\lambda}\sigma_{xx0}^{(90^\circ)}\frac{\mathrm{d}\phi(\xi)}{\mathrm{d}\xi}(h/t_1-\omega), \\
\sigma_{22}^{(90^\circ)} &= \sigma_{yy0}^{(90^\circ)} \\
\sigma_{22}^{(0^\circ)} &= \sigma_{yy0}^{(0^\circ)} \\
\sigma_{33}^{(90^\circ)} &= \frac{1}{2}\sigma_{xx0}^{(90^\circ)}\frac{\mathrm{d}^2\phi(\xi)}{\mathrm{d}\xi^2}[h/t_1-\omega^2] \\
\sigma_{33}^{(0^\circ)} &= \frac{1}{2\lambda}\sigma_{xx0}^{(90^\circ)}\frac{\mathrm{d}^2\phi(\xi)}{\mathrm{d}\xi^2}[h/t_1-\omega]^2.
\end{aligned} \tag{27}$$

Stresses used in eqns (17)–(26) are written below as functions of ξ and ω

$$\sigma_{\alpha\alpha}^{(90^\circ)} = \sigma_{\alpha\alpha}^{(90^\circ)}(\xi,\omega) = \sigma_{11}^{(90^\circ)} + \sigma_{22}^{(90^\circ)} + \sigma_{33}^{(90^\circ)}$$

$$\sigma_{11}^{*\,(90^\circ)} = \sigma_{11}^{*\,(90^\circ)}(\xi,\omega) = \sigma_{11}^{(90^\circ)}(\xi,\omega) - \tfrac{1}{3}\sigma_{\alpha\alpha}^{(90^\circ)}$$

$$\sigma_{22}^{*\,(90^\circ)} = \sigma_{22}^{*\,(90^\circ)}(\xi,\omega) = \sigma_{22}^{(90^\circ)}(\xi,\omega) - \tfrac{1}{3}\sigma_{\alpha\alpha}^{(90^\circ)}$$

$$\sigma_{33}^{*\,(90^\circ)} = \sigma_{33}^{*\,(90^\circ)}(\xi,\omega) = \sigma_{33}^{(90^\circ)}(\xi,\omega) - \tfrac{1}{3}\sigma_{\alpha\alpha}^{(90^\circ)}$$

$$\sigma_{13}^{*\,(90^\circ)} = \sigma_{13}^{(90^\circ)}(\xi,\omega) = \omega\sigma_{xx0}^{(90^\circ)}\frac{\mathrm{d}\phi(\xi)}{\mathrm{d}\xi}$$

$$\sigma^{eff\,90^\circ} = \sigma^{eff,\,90^\circ}(\xi,\omega)$$
$$= \{\tfrac{3}{2}[(\sigma_{11}^{*\,(90^\circ)})^2 + (\sigma_{22}^{*\,(90^\circ)})^2 + (\sigma_{33}^{*\,(90^\circ)})^2 + (\sigma_{13}^{*\,(90^\circ)})^2]\}^{0.5}$$

$$\sigma_{\alpha\alpha}^{(0^\circ)} = \sigma_{\alpha\alpha}^{(0^\circ)}(\xi,\omega) = \sigma_{11}^{(0^\circ)} + \sigma_{22}^{(0^\circ)} + \sigma_{33}^{(0^\circ)}$$

$$\sigma_{11}^{*\,(0^\circ)} = \sigma_{11}^{*\,(0^\circ)}(\xi,\omega) = \sigma_{11}^{(0^\circ)}(\xi,\omega) - \tfrac{1}{3}\sigma_{\alpha\alpha}^{(0^\circ)}$$

$$\sigma_{22}^{*\,(0^\circ)} = \sigma_{22}^{*\,(0^\circ)}(\xi,\omega) = \sigma_{22}^{(0^\circ)}(\xi,\omega) - \tfrac{1}{3}\sigma_{\alpha\alpha}^{(0^\circ)}$$

$$\sigma_{33}^{*\,(0^\circ)} = \sigma_{33}^{*\,(0^\circ)}(\xi,\omega) = \sigma_{33}^{(0^\circ)}(\xi,\omega) - \tfrac{1}{3}\sigma_{\alpha\alpha}^{(0^\circ)}$$

$$\sigma_{13}^{*\,(0^\circ)} = \sigma_{33}^{(0^\circ)}(\xi,\omega) = \frac{1}{\hat{\lambda}}\sigma_{xx0}^{(90^\circ)}\frac{\mathrm{d}\phi(\xi)}{\mathrm{d}\xi}(h/t_1 - \omega)$$

$$\sigma^{eff,0^\circ} = \sigma^{eff,0^\circ}(\xi,\omega)$$
$$= \{\tfrac{3}{2}[(\sigma_{11}^{*\,(0^\circ)})^2 + (\sigma_{22}^{*\,(0^\circ)}) + (\sigma_{33}^{*\,(0^\circ)})^2 + (\sigma_{13}^{*\,(0^\circ)})^2]\}^{0.5}. \tag{28}$$

Using eqns (25), (26) and (28), the inelastic strains (creep strains in the present case), $\varepsilon_{ij}^{c(90^\circ)}$ and $\varepsilon_{ij}^{c(0^\circ)}$ are expressed in terms of ω, ξ and $\phi(\xi)$. The inhomogeneous term $F(\xi)$ of the governing equation, eqn (13), is then expressed in terms of ξ and $\phi(\xi)$ using eqns (7)–(12). The problem is therefore converted to the nonlinear differential equation, eqn (13), which we proceed to solve by constructing the Green's function of the linear homogeneous equation.

THE GREEN'S FUNCTION

The proposed problem of analyzing a laminate with cracked 90° plies and inelastic strains is reduced to solving eqn (13) for the stress function, $\phi(\xi)$. Since the inhomogeneous term, $F(\xi)$, in eqn (13) is a function of inelastic strain which depends on time and stress history, an incremental analysis is needed to determine the stress function, $\phi(\xi)$, during the loading and unloading process. For this purpose the Green's function for the system is constructed. We seek the solution of the following boundary value problem

$$\frac{\mathrm{d}^4 G(\xi,\eta)}{\mathrm{d}\xi^4} + p\frac{\mathrm{d}^2 G(\xi,\eta)}{\mathrm{d}\xi^2} + qG(\xi,\eta) = \delta(\xi-\eta) \tag{29}$$

$$G(\xi,\eta)|_{\xi=\pm\rho} = 0, \quad \frac{\mathrm{d}G}{\mathrm{d}\xi}(\xi,\eta)|_{\xi=\pm\rho} = 0 \tag{30}$$

where $\delta(\xi-\eta)$ is the Dirac delta function.

The solution to eqn (29) with the boundary conditions in eqn (30) can be obtained by the following heuristic procedure. Let ϕ_1 and ϕ_2 be two general solutions of the homogeneous equation

$$\frac{d^4\phi(\xi)}{d\xi^4} + p\frac{d^2\phi(\xi)}{d\xi^2} + q\phi(\xi) = 0 \tag{31}$$

where ϕ_1 satisfies the boundary conditions at $\xi = -\rho$ and ϕ_2 satisfies the boundary conditions at $\xi = \rho$, i.e.,

$$\phi_1(\xi)|_{\xi=-\rho} = 0, \quad \left.\frac{d\phi_1(\xi)}{d\xi}\right|_{\xi=-\rho} = 0; \quad \phi_2(\xi)|_{\xi=\rho} = 0, \quad \left.\frac{d\phi_2(\xi)}{d\xi}\right|_{\xi=\rho} = 0.$$

If ϕ_1 and ϕ_2 also satisfy the conditions at $\xi = \eta$,

$$\phi_1(\xi)|_{\xi=\eta} = \phi_2(\xi)|_{\xi=\eta}, \quad \left.\frac{d\phi_1(\xi)}{d\xi}\right|_{\xi=\eta} = \left.\frac{d\phi_2(\xi)}{d\xi}\right|_{\xi=\eta}$$

$$\left.\frac{d^2\phi_1(\xi)}{d\xi^2}\right|_{\xi=\eta} = \left.\frac{d^2\phi_2(\xi)}{d\xi^2}\right|_{\xi=\eta}, \quad \left.\frac{d^3\phi_1(\xi)}{d\xi^3}\right|_{\xi=\eta} = \left.\frac{d^3\phi_2(\xi)}{d\xi^3}\right|_{\xi=\eta} - 1 \tag{32}$$

then

$$G(\xi,\eta) = \begin{cases} \phi_1(\xi) & \text{for } \xi \leqslant \eta \\ \phi_2(\xi) & \text{for } \xi > \eta \end{cases}$$

is the Green's function for the problem. It is not difficult to show that the $G(\xi,\eta)$ constructed above satisfies eqns (29) and (30), and therefore, is the Green's function for the problem. First, $G(\xi,\eta)$ satisfies the boundary conditions at $\xi = -\rho$ and $\xi = \rho$ since $\phi_1(\xi)$ and $\phi_2(\xi)$ satisfy the boundary conditions at $\xi = -\rho$ and $\xi = \rho$, respectively. Secondly, $G(\xi,\eta)$ satisfies the homogeneous equation corresponding to eqn (29) for any $\xi \neq \eta$ because both $\phi_1(\xi)$ and $\phi_2(\xi)$ are solutions of the homogeneous equation. Finally, using condition in eqn (32), eqn (29) is integrated to obtain

$$\lim_{\varepsilon\to 0}\int_{\eta-\varepsilon}^{\eta+\varepsilon} [\text{Left hand side}]\,d\xi = \lim_{\varepsilon\to 0}\int_{\eta-\varepsilon}^{\eta+\varepsilon}\left[\frac{d^4G(\xi,\eta)}{d\xi^4} + p\frac{d^2G(\xi,\eta)}{d\xi^2} + qG(\xi,\eta)\right]d\xi$$

$$= \left[\frac{d^3G(\eta+\varepsilon,\eta)}{d\xi^3} - \frac{d^3G(\eta-\varepsilon,\eta)}{d\xi^3}\right] + p\left[\frac{dG(\eta+\varepsilon,\eta)}{d\xi} - \frac{dG(\eta-\varepsilon,\eta)}{d\xi}\right] + \lim_{\varepsilon\to 0}\int_{\eta-\varepsilon}^{\eta+\varepsilon} qG(\xi,\eta)\,d\xi$$

$$= \left[\frac{d^3\phi_2(\eta)}{d\xi^3} - \frac{d^3\phi_1(\eta)}{d\xi^3}\right] + p\left[\frac{d\phi_2(\eta)}{d\xi} - \frac{d\phi_1(\eta)}{d\xi}\right]$$

$$= 1 = \lim_{\varepsilon\to 0}\int_{\eta-\varepsilon}^{\eta+\varepsilon}\delta(\xi-\eta)\,d\xi = \lim_{\varepsilon\to 0}\int_{\eta-\varepsilon}^{\eta+\varepsilon}[\text{right hand side}]\,d\xi.$$

The limit, $\lim_{\varepsilon\to 0}\int_{\eta-\varepsilon}^{\eta+\varepsilon} qG(\xi,\eta)\,d\xi$, in the above equation, is equal to zero since $G(\xi,\eta)$ is continuous. The above procedure of determining the Green's function in eqn (29) is an extension of the approach described by Stakgold (1970).

It can be verified that ϕ_1 and ϕ_2 take the following form

$$\phi_1(\xi) = -b_1u_1(\xi) - b_2u_2(\xi)$$
$$\phi_2(\xi) = b_3u_3(\xi) + b_2u_4(\xi) \tag{33}$$

where the unknown constants b_1, b_2, b_3 and b_4 (they are actually related to η) are to be determined from the matching conditions at $\xi = \eta$, eqn (32). Functions $u_1(\xi)$ and $u_2(\xi)$ are

the solutions for the homogeneous equation, eqn (31), and satisfy the homogeneous boundary conditions at $\xi = -\rho$, i.e.,

$$u_1(\xi)|_{\xi=-\rho} = \left.\frac{du_1(\xi)}{d\xi}\right|_{\xi=-\rho} = u_2(\xi)|_{\xi=-\rho} = \left.\frac{du_2(\xi)}{d\xi}\right|_{\xi=-\rho} = 0.$$

Similarly, $u_3(\xi)$ and $u_4(\xi)$ are also the solutions of eqn (31) and satisfy the homogeneous boundary conditions at $\varepsilon = \rho$. The forms of $u_1(\xi)$, $u_2(\xi)$, $u_3(\xi)$ and $u_4(\xi)$ depend on the values of p and q as discussed in Appendix B. When $(p^2/4) - q < 0$ (see eqns (B7) and (B8))

$$\begin{aligned}
u_1(\xi) &= \sinh[\alpha(\xi+\rho)]\sin[\beta(\xi+\rho)] \\
u_2(\xi) &= \cosh[\alpha(\xi+\rho)]\sin[\beta(\xi+\rho)] - \frac{\beta}{\alpha}\sinh[\alpha(\xi+\rho)]\cos[\beta(\xi+\rho)] \\
u_3(\xi) &= \sinh[\alpha(\xi-\rho)]\sin[\beta(\xi-\rho)] \\
u_4(\xi) &= \cosh[\alpha(\xi-\rho)]\sin[\beta(\xi-\rho)] - \frac{\beta}{\alpha}\sinh[\alpha(\xi-\rho)]\cos[\beta(\xi-\rho)]
\end{aligned} \tag{34}$$

where

$$\alpha = \frac{\sqrt{-p+2\sqrt{q}}}{2} \quad \text{and} \quad \beta = \frac{\sqrt{p+2\sqrt{q}}}{2}. \tag{35}$$

Derivation of eqns (34) and (35) as well as the expressions of $u_1(\xi)$, $u_2(\xi)$, $u_3(\xi)$ and $u_4(\xi)$ for other values of p and q can be found in Appendix B.

Substituting eqns (33), (34) and (35) into eqn (32), one obtains the following condition to determine the constants b_1, b_2, b_3 and b_4

$$\begin{bmatrix} u_1(\eta) & u_2(\eta) & u_3(\eta) & u_4(\eta) \\ u_1'(\eta) & u_2'(\eta) & u_3'(\eta) & u_4'(\eta) \\ u_1''(\eta) & u_2''(\eta) & u_3''(\eta) & u_4''(\eta) \\ u'''_1(\eta) & u'''_2(\eta) & u'''_3(\eta) & u'''_4(\eta) \end{bmatrix} \begin{Bmatrix} b_1 \\ b_2 \\ b_3 \\ b_4 \end{Bmatrix} = \begin{Bmatrix} 0 \\ 0 \\ 0 \\ 1 \end{Bmatrix} \tag{36}$$

where prime denotes the derivative with respect to η. By solving the above system of algebraic equations for b_1, b_2, b_3 and b_4, one obtains

$$\begin{aligned}
b_1 &= b_1(\eta) = -W[u_2(\eta), u_3(\eta), u_4(\eta)]/W[u_1(\eta), u_2(\eta), u_3(\eta), u_4(\eta)] \\
b_2 &= b_2(\eta) = W[u_1(\eta), u_3(\eta), u_4(\eta)]/W[u_1(\eta), u_2(\eta), u_3(\eta), u_4(\eta)] \\
b_3 &= b_3(\eta) = -W[u_1(\eta), u_2(\eta), u_4(\eta)]/W[u_1(\eta), u_2(\eta), u_3(\eta), u_4(\eta)] \\
b_4 &= b_4(\eta) = W[u_1(\eta), u_2(\eta), u_3(\eta)]/W[u_1(\eta), u_2(\eta), u_3(\eta), u_4(\eta)]
\end{aligned} \tag{37}$$

where $W[\ldots]$ is the Wronskian of the function involved. For example,

$$W[u_1(\eta), u_2(\eta), u_3(\eta), u_4(\eta)] = \det \begin{bmatrix} u_1(\eta) & u_2(\eta) & u_3(\eta) & u_4(\eta) \\ u_1'(\eta) & u_2'(\eta) & u_3'(\eta) & u_4'(\eta) \\ u_1''(\eta) & u_2''(\eta) & u_3''(\eta) & u_4''(\eta) \\ u'''_1(\eta) & u'''_2(\eta) & u'''_3(\eta) & u'''_4(\eta) \end{bmatrix} \tag{38}$$

and

$$W[u_2(\eta), u_3(\eta), u_4(\eta)] = \det\begin{pmatrix} u_2(\eta) & u_3(\eta) & u_4(\eta) \\ u_2'(\eta) & u_3'(\eta) & u_4'(\eta) \\ u_2''(\eta), & u_3''(\eta) & u_4''(\eta) \end{pmatrix}, \text{etc}$$

where det denotes the determinant of a matrix. From the property of the Green's function the solution of eqn (13) is then given as

$$\phi(\xi) = \phi_0(\xi) + \int_{-\rho}^{\rho} F(\eta) G(\xi, \eta)\, d\eta \tag{39}$$

where $\phi_0(\xi)$ is the solution of the homogeneous equation (with $F(\xi) = 0$ in eqn (13)) under the boundary condition shown in eqn (14), and is given as, for $(p^2/4) - q < 0$ (see eqn (B9))

$$\phi_0(\xi) = \frac{2(\beta \sinh[\alpha\rho]\cos[\beta\rho] + \alpha \cosh[\alpha\rho]\sin[\beta\rho])}{\beta \sinh[2\alpha\rho] + \alpha \sin[2\beta\rho]} \cosh[\alpha\xi]\cos[\beta\xi] + \frac{2(\beta \cosh[\alpha\rho]\sin[\beta\rho] - \alpha \sinh[\alpha\rho]\cos[\beta\rho])}{\beta \sinh[2\alpha\rho] + \alpha \sin[2\beta\rho]} \sinh[\alpha\xi]\sin[\beta\xi]. \tag{40}$$

Derivation of eqn (40) as well as the expressions of $\phi_0(\xi)$ for other values of p and q can be found in Appendix B.

PROCEDURE FOR SOLUTION

The procedure for solving the stress function, $\phi(\xi)$, is as follows:

(1) At the start of the first time interval, ε_{ij}^c is zero. From eqns (7)–(13), one finds that

$$F(\xi) = \frac{(\alpha_T - \alpha_A)\,\Delta T}{C_3}.$$

The stress function in eqn (13) with the above inhomogeneous term, $F(\xi)$, is constructed as

$$\phi(\xi) = \left(1 - \frac{(\alpha_T - \alpha_A)\,\Delta T}{C_3}\right)\phi_0(\xi) + \frac{(\alpha_T - \alpha_A)\,\Delta T}{C_3}.$$

(2) The stress components are then derived from eqns (27) and (28) using the stress function obtained above. The approximation of stress is then substituted into eqns (25) and (26) to obtain the incremental creep strains, $\Delta\varepsilon_{ij}^{c(90°)}$ and $\Delta\varepsilon_{ij}^{c(0°)}$.

(3) The incremental creep strains, $\Delta\varepsilon_{ij}^{c(90°)}$ and $\Delta\varepsilon_{ij}^{c(0°)}$, are added to the creep strains accumulated during all previous steps, $\varepsilon_{ij}^{co(90°)}$ and $\varepsilon_{ij}^{co(0°)}$, to obtain the total creep strains, i.e. $\varepsilon_{ij}^{c(90°)} = \varepsilon_{ij}^{co(90°)} + \Delta\varepsilon_{ij}^{c(90°)}$ and $\varepsilon_{ij}^{c(0°)} = \varepsilon_{ij}^{co(0°)} + \Delta\varepsilon_{ij}^{c(0°)}$. For the first iteration step $\varepsilon_{ij}^{co(90°)} = \Delta\varepsilon_{ij}^{c(90°)}$, and $\varepsilon_{ij}^{co(0°)} = \Delta\varepsilon_{ij}^{c(0°)}$ because $\varepsilon_{ij}^{co(90°)}$ and $\varepsilon_{ij}^{co(0°)}$ are zero.

(4) The above creep strain is substituted into eqns (7)–(13) to obtain $A_1(\xi)$, $B_1(\xi)$, etc. and then $F(\xi)$. The stress function is then obtained as

$$\phi(\xi) = \phi_0(\xi) + \int_{-\rho}^{\rho} F(\eta) G(\xi, \eta)\, d\eta. \tag{41}$$

(5) The creep strain at the beginning of next time interval is known and is equal to the accumulated incremental strains up to the time interval. The procedure for calculating the stress function, stresses and displacements for the other time interval is the same as in steps 2 to 4.

Table 1. Material properties of the unidirectional laminate

E_A	E_T	G_A	G_T	ν_T	ν_A
109 GPa	14.6 GPa	6.26 GPa	6.18 GPa	0.1878	0.236

RESULTS

As an example of the utility of the method, we will model the creep response of the eight-harness satin weave (8HSW) Nextel 610/Aluminosilicate ceramic matrix composite which has been experimentally studied by Lee *et al.* (1996). Creep tests have been conducted at 1000°C and 1100°C at stresses ranging from 50 MPa to 135 MPa. The ply properties are given in Table 1. The creep behavior of the 0° plies is dominated by the fibers and the creep behavior of 90° plies is dominated by the matrix. Therefore, n_f in the constitutive model, eqn (23), is taken as 3 after Wilson *et al.* (1993) for that of the fibers, and n_m is taken as 4 after Zuiker (1996) for that of the matrix. Due to the lack of experimental data on creep of the matrix it is assumed that $w_f = w_m = 2.13821 \times 10^{-14}$ using the data on total strain at time equal to 1000 seconds at the load level of 75 MPa from the creep tests on the composite (Lee *et al.*, 1996). The same w_f and w_m are used in the prediction of the curve for the load level of 50 MPa. Figure 2 shows the comparison of the total strain of the composite at 1100°C under two loads levels, $\sigma_{\text{applied}} = 50$ MPa and $\sigma_{\text{applied}} = 75$ MPa. Although Fig. 2 shows that the predicted creep strains agree with experiments at different stress levels reasonably well, it should not be considered to be the definitive verification of the proposed model due to the lack of experimental data of the matrix.

The creep strains, average in the z-direction, of the 0° and 90° plies, after 7200 seconds, are shown in Fig. 3 as functions of the distance from the crack face of two adjacent matrix cracks, one at $x/t_1 = -2$, the other at $x/t_1 = 2$. The crack spacing a is chosen to be $2t_1$, in agreement with observations of processing induced cracks in the composite (Lee *et al.*, 1996), where t_1 is the thickness of one 90° ply. The applied stress and temperature on the composite are 75 MPa and 1100°C, respectively. As shown in Fig. 3, the creep strain of the 90° plies is negligibly small when compared to that of the 0° plies. Since the total strains of the 0° and 90° plies are equal to maintain the global deformation compatibility, the deformation caused by crack opening of the 90° plies is considerable. For both 90° and 0° plies, the maximum creep strain occurs at $x/t_1 = -2$ and $x/t_1 = 2$, the crack surface, indicating the influence of the crack on creep deformation is most significant on crack surface.

A three-dimensional distribution of axial creep strains, ε_{11}^c or ε_{xx}^c, in the 0° plies after 12,000 seconds is shown in Fig. 4 where z and x are the directions along the thickness direction and axial direction (x-direction) as shown in Fig. 1. Focusing the attention to the distribution of the creep strain of the 0° plies on the planes where z is constant, one finds

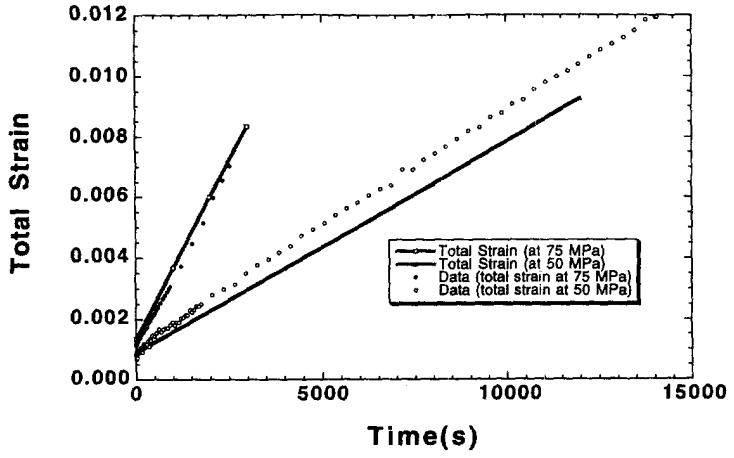

Fig. 2. Comparison of predicted strains with experimental data.

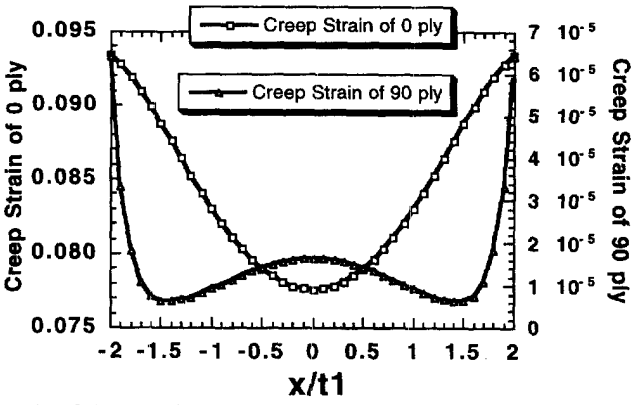

Fig. 3. Creep strain of the 0° and 90° plies averaged along the thickness direction (z-direction in Fig. 1).

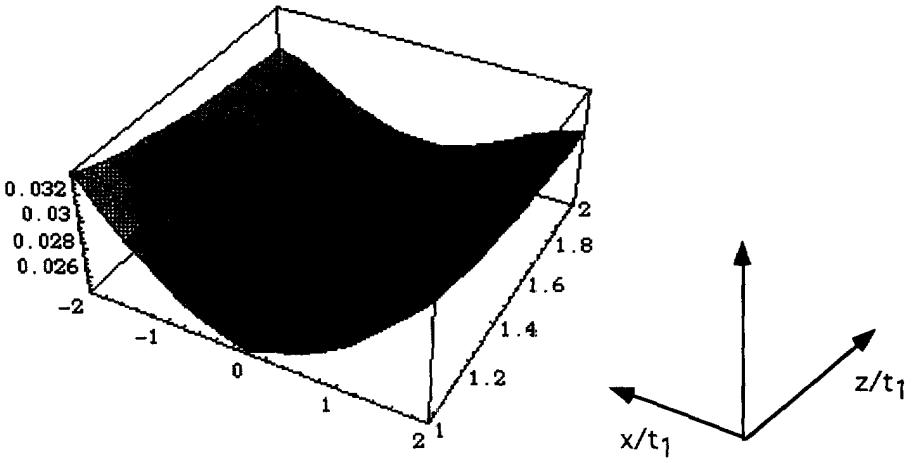

Fig. 4. Axial creep strains, ε_{11}^{c} or ε_{xx}^{c}, in the 0° plies.

that on $z = 1$ where 90° and 0° plies meet, the creep strain exhibits largest variation along the axial direction. This indicates that on $z = 1$, the effect of the cracks is most significant to the 0° plies since the variation of the creep strain in the 0° plies is a direct result of the cracks in the 90° plies. On other planes where z is constant, as the value of z increases, the material is further away from the cracked 90° plies, and the effect of the cracks becomes less significant. Hence, the variation of the creep strain becomes smaller. A three-dimensional distribution of axial creep strains, ε_{11}^{c} or ε_{xx}^{c}, in the 90° plies after 12,000 seconds is shown in Fig. 5. One advantage of the present analysis is the ability to obtain stress and strain variations along both axial and thickness directions rather than average stress and strain.

The normal stresses along the loading direction in the 0° plies (i.e., $\sigma_{xx}^{(0^\circ)}$) and 90° plies (i.e., $\sigma_{xx}^{(90^\circ)}$), under an applied load of 75 MPa after 12,000 seconds at a constant temperature of 1100°C, are shown in Fig. 6. These normal stresses have no dependence on z, and are normalized by $\sigma_{xx0}^{(90^\circ)}$, the stress of the 90° plies from the linear classic laminate analysis when no matrix cracks and inelastic deformation are considered. On the crack surface, $x/t_1 = -2$ and $x/t_1 = 2$, $\sigma_{xx}^{(90^\circ)}$ is zero and $\sigma_{xx}^{(0^\circ)}$ arrives at its maximum value to balance the applied load. When moving to the center of the two cracks, $\sigma_{xx}^{(90^\circ)}$ beings to increase and $\sigma_{xx}^{(0^\circ)}$ starts to decrease. The maximum value of $\sigma_{xx}^{(90^\circ)}$ is about 40% of the normal stress in the 90° plies in the undamaged composite. Furthermore, due to the relatively large creep strain in the 0° ply, relaxation in the 0° ply occurs which reduces the magnitude of the stress as compared to the elastic stress also shown in Fig. 6. The elastic stress is the stress of the composite at time equal to zero when cracks exist in the 90° plies, but no creep deformation has occurred. The stress in the 90° plies increases as creep strain develops. The stress changes

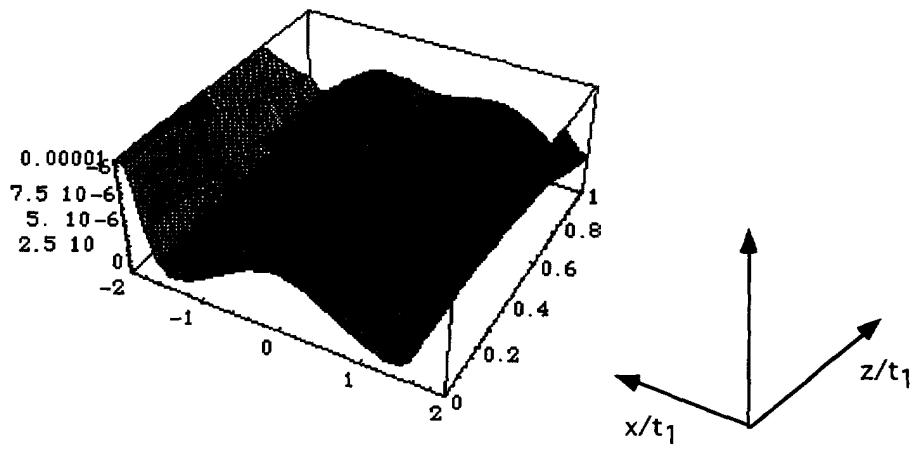

Fig. 5. Axial creep strains, ε_{11}^{c} or ε_{xx}^{c}, in the 90° plies.

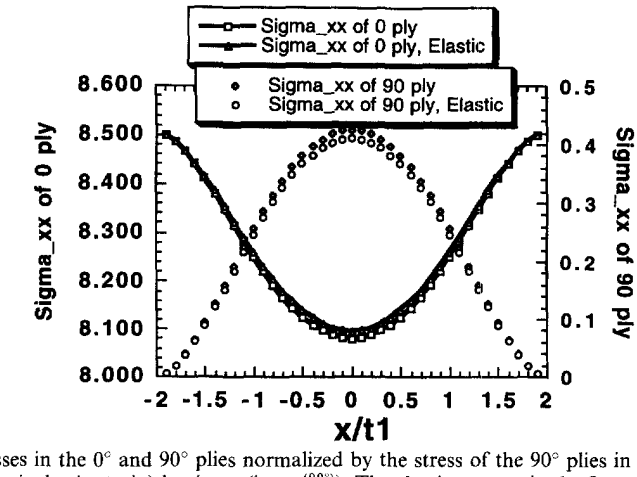

Fig. 6. Stresses in the 0° and 90° plies normalized by the stress of the 90° plies in the undamaged (no crack, no inelastic strain) laminate (i.e., $\sigma_{xx0}^{(90^\circ)}$). The elastic stresses in the figure are the stresses in the composite at time equal to zero when cracks exist in the 90° plies, but no inelastic strain has been developed.

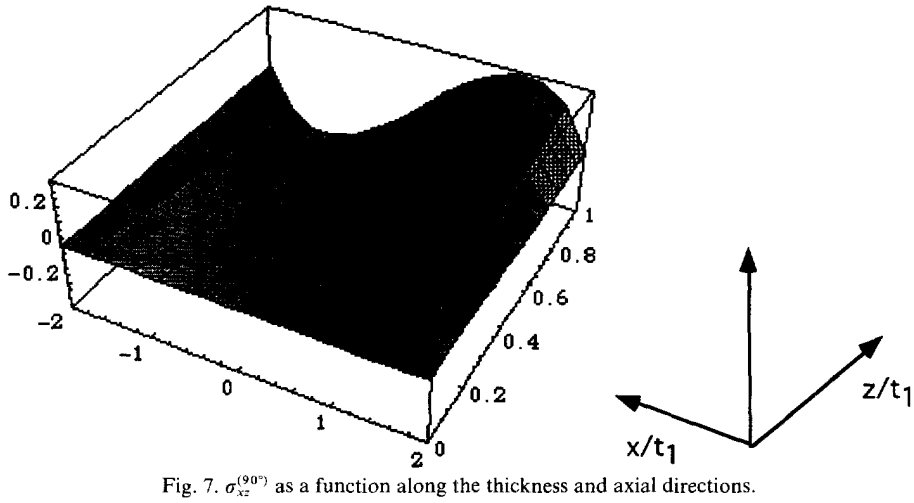

Fig. 7. $\sigma_{xz}^{(90^\circ)}$ as a function along the thickness and axial directions.

in the 0° and 90° plies, and the stress transfer from between these two plies are expected to be more pronounced over a longer period of time.

The transverse shear stresses of the 90° plies, $\sigma_{xz}^{(90^\circ)}$, is a function along the thickness and axial directions, and is shown in Fig. 7. The shear stress is zero at $z = 0$ due to symmetry

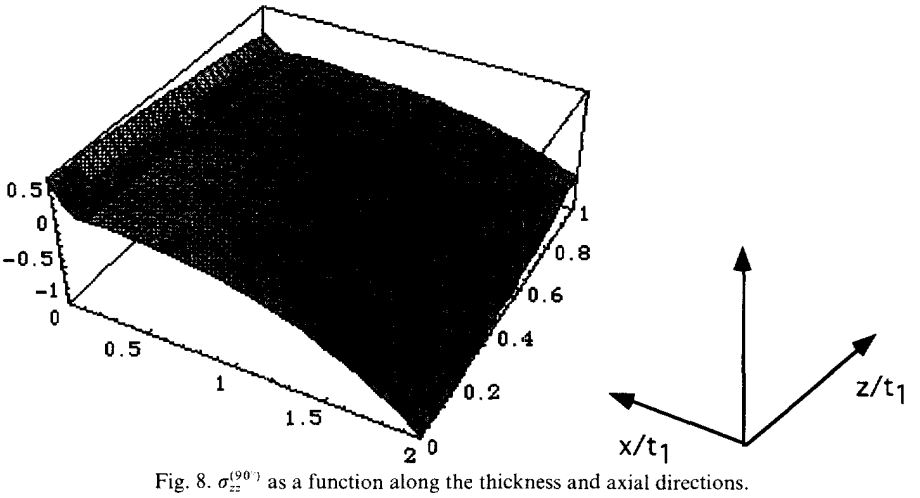

Fig. 8. $\sigma_{zz}^{(90^\circ)}$ as a function along the thickness and axial directions.

and at the crack surface due to the traction free condition. The normal stress of the 90° plies, $\sigma_{zz}^{(90^\circ)}$, is shown in Fig. 8.

CONCLUSION

A general framework for the analysis of cross-ply laminates with matrix cracks and inelastic deformation is proposed. The stress and strain states in the composites are represented through a simple integral of the Green's function and the inelastic strains accumulated in the previous time steps. This new analysis takes into consideration the crack–crack interaction, as well as crack–inelastic deformation interaction. The method predicts variation in the stress and strain fields between cracks. In addition, the predicted stress field satisfies equilibrium and all boundary and interface conditions. The compatibility equations of continuum are satisfied approximately by minimizing the complementary energy of the composite material. One possible improvement on accuracy one can make to the present analysis is to enlarge the admissible stress field for the variational principle. Such an attempt will most likely complicate the analysis significantly and eliminate the possibility of an analytical or semi-analytical solution.

The present model has been utilized to study the interactions of matrix cracks and creep deformation in a ceramic matrix composite. The results show important variations of stress and strain fields along both thickness and axial directions. The predicted creep strain of the composite shows good correlation with experimental data at different levels of temperature and stress conditions.

We still should consider the consequences of the one assumption that the x direction normal stresses in each ply are independent of z. With this assumption, we miss microcrack tip stress concentration effects. At high loads the tips of microcracks can lead to delamination between the 0° and 90° plies. The prediction of creep strains and stresses at near the crack tips is not accurate, and should be interpreted as the average value through the thickness, z, direction. It should be pointed out, however, that many analytical or semi-analytical models on composite materials involving inelastic deformation are based on Eshelby's concept of equivalent inclusion which gives only average stresses and strains in the whole matrix material. These models have been shown to represent the average total strain including creep strain of the composite reasonably close to experimental measurements (Mura, 1987; Taya and Mori, 1987; Zhu and Weng, 1990). The model proposed in this paper is suitable for a cross-ply laminate only, but it represents an improvement to the equivalent inclusion approach in regards to local stress and strain fields.

Acknowledgements—The authors wish to thank Mr Dave Johnson for helping with the Mathematica program used in the calculation of the report. Support of AFOSR to the first author through the Summer Faculty Research Program is gratefully acknowledged. Finally, the authors would like to thank two unidentified reviewers for valuable comments and suggestions.

REFERENCES

Aboudi, J. (1991) *Mechanics of Composite Materials: A Unified Micromechanical Approach.* Elsevier, Amsterdam.

Bahei-El-Din, Y. A. (1990) Thermal and mechanical behavior of ceramic and metal matrix composites, eds J. M. Kennedy, H. H. Hoeller and W. S. Johnson. ASTM STP 1080, ASTM, Philadelphia, pp. 20–39.

Bahei-El-Din, Y. A. and Dvorak, G. J. (1989) A review of plasticity theory of fibrous composite materials. In *Metal Matrix Composites: Testing, Analysis, and Failure Modes*, ASTM STP 1032, ASTM, Philadelphia, pp. 103–129.

Bailey, J. E., Curtis, P. T. and Parvizi, A. (1979) On the transverse cracking and longitudinal splitting behavior of glass and carbon fibre reinforced epoxy cross ply laminates and the effect of Poisson and thermally generated strain. *Proceedings of the Royal Society of London*, A366. **16,** 599–623.

Coker, D., Ashbaugh, N. E. and Nicholas, T. (1993) Analysis of thermomechanical cyclic behavior of unidirectional metal matrix composites. *Thermomechanical Fatigue Behavior of Materials*, ASTM STP 1186, eds H. Sehitoglu. American Society for Testing and Materials, Philadelphia, pp. 50–59.

Dvorak, G. J. (1991) Plasticity theories for fibrous composite materials. In *Metal Matrix Composite Materials, Mechanisms and Properties*, Vol. 2, pp. 1–77. Academic Press. Boston.

Dvorak, G. J. and Bahei-El-Din, Y. A. (1982) Plasticity analysis of fibrous composites. *Journal of Applied Mechanics* **49,** 327–335.

Dvorak, G. J. and Teply, Y. (1985) Periodic hexagonal array models for plasticity analysis of composite materials. In *Plasticity Today: Modelling, Methods, and Applications*, 623–641.

Flaggs, D. L. (1985) Prediction of tensile matrix failure in composite laminates. *Journal of Composite Materials* **19,** 29–50.

Hashin, Z. (1985) Analysis of cracked laminates: a variational approach. *Mechanics of Materials* **4,** 121–136.

Hashin, Z. (1987) Analysis of orthogonally cracked laminates under tension. *Journal of Applied Mechanics* **54,** 872–879.

Highsmith, A. L. and Reifsnider, K. L. (1982) Stiffness-reduction mechanisms in composite laminates. *Damage in Composite Materials*, ASTM STP 775, eds K. L. Reifsnider. American Society for Testing and Materials, 1982, pp. 103–117.

Ishikawa, T. and Chou, T. W. (1983) One-dimensional micromechanical analysis of woven fabric composites. *AIAA Journal* **21,** 1714–1721.

Krempl, E. and Hong, B. Z. (1989) A simple laminate theory using the orthotropic viscoplasticity theory based on overstress. Part I: in-plane stress–strain relationships for metal matrix composites. *Composites Science Technology* **35,** 53–74.

Kroupa, J. L., Neu, R. W., Nicholas, T., Coker, D., Robertson, D. D. and Mall, S. (1996) A comparison of analysis tools for predicting the inelastic cyclic response of cross-ply titanium matrix composites. In *Life Prediction Methodology for Titanium Matrix Composites*. ASTM STP 1253, ASTM, Philadelphia.

Laws, N., Dvorak, G. J. and Hejazi, M. (1983) Stiffness changes in unidirectional composites caused by crack systems. *Mechanics of Materials* **2,** 123–137.

Lee, S. S., Zawada, L. P., Hay, R., Staehler, J. and Carper, D. M. (1996) Mechanical behavior and high temperature long-term performance of an oxide–oxide ceramic matrix composite. *Journal of American Ceramic Society* (submitted).

McCartney, L. N. (1992) Theory of stress transfer in a 0°–90°–0° cross-ply laminate containing a parallel array of transverse cracks. *Journal of Mechanics and Physics of Solids* **40**(1), 27–68.

Mukherjee, A. K., Bird, J. E. and Dorn, J. E. (1969) *ASM Transaction Quarterly*, **62,** 155–179.

Mura, T. (1987) *Micromechanics of Defects in Solids* (2nd edn). Martinus Nijhoff, Dordrecht.

Narin, J. A. (1989) The strain energy release rate of composite microcracking: a variational approach. *Journal of Composite Materials* **23,** 1106–1124.

Parvizi, A., Garrett, K. W. and Bailey, J. E. (1978) Constrained cracking in glass fibre-reinforced epoxy cross-ply laminates, *Journal of Material Science* **13,** 195–201.

Stakgold, Ivar (1970) *Boundary Value Problems of Mathematical Physics, Vol. I.* The Macmillan Company, Collier–MacMillan Limited, London, pp. 63.

Talreja, R. (1985) Transverse cracking and stiffness reduction in composite laminates. *Journal of Composite Materials* **19,** 355–375.

Taya, M. and Mori, T. (1987) *Proceedings of the IUTAM Symposium: Thermo-Mechanical Couplings in Solids.* Elsevier Science, Oxford, pp. 147–162.

Teply, J. and Dvorak, G. J. (1988) Bounds on overall instantaneous properties of elastic–plastic composites. *Journal of the Mechanics and Physics of Solids* **36,** 29–58.

Wilson, D. M., Lueneburg, D. C. and Lieder, S. L. (1993) High temperature properties of Nextel 610 and alumina-based nanocomposites fibers. *Ceramic Engineering Science Proceedings* **14**(7-8), 609–621.

Zhu, Z. G. and Weng, G. J. (1990) Creep anisotropy of a metal-matrix composite containing dilute concentration of aligned spheroidal inclusions. *Mechanics of Materials* **9,** 93–105.

Zuiker, J. R. (1996) Modeling the creep response of ceramic matrix composites: a tool for inferring in-situ matrix properties. *Thermal and Mechanical Testing Methods and Behavior of Continuous-Fiber Ceramic Composites*, ASTM STP 1309, ASTM, Philadelphia (to appear).

APPENDIX A

McCartney (1992) has developed two new analytical methods that can predict the stress transfer between the 0° and 90° plies in a cross-ply laminate containing transverse cracks using the general framework of 2-D and 3-D elasticity. The first method is based on a 2-D model which assumes that generalized plane strain condition prevails in the XZ plane. The theoretical approach retains all relevant stress and displacement components, and satisfy exactly the equilibrium equation, the interface conditions and other conditions involving stresses. The stress–strain relations are satisfied either exactly or in an averaged sense. The second analytical method extends the 2-D

model so that it can apply to 3-D problems which arise, for example when edge effects or orthogonal cracking are taken into account.

In McCartney's 2-D model, the displacements are $u = u(x, z)$, $x = Ay$, $w = w(x, z)$. Here A is a constant. It follows from the displacements that the shear stresses σ_{yz} and σ_{xy} are zero. McCartney (1992) has shown that the 2-D model, when the axial stress in 0 and 90 plies are assumed independent of the through-thickness coordinate, z, are equivalent to the Euler equation from Hashin's variational analysis. Therefore, eqn (1) represents a general stress field in the framework of the generalized plane strain condition with addition of one assumption that the σ_{xx} is a function of x only.

Equation (1) can be modified to introduce a 3-D stress representation with nonzero σ_{yz} and σ_{xy}, using the approach outlined by Hashin (1987). The method proposed in this paper can still be applied without much change.

APPENDIX B

In this appendix, the general solution of eqn (31) is discussed, and the expressions of $u_1(\xi)$, $u_2(\xi)$, $u_3(\xi)$ and $u_4(\xi)$, used in eqn (33) for the construction of the Green's function, are provided.

Equation (31) becomes

$$k^4 + pk^2 + qk = 0 \tag{B1}$$

if $\phi(\xi)$ is assumed to be in the form of $e^{k\xi}$. The roots for eqn (B1) are

$$k = k_1 = \sqrt{\frac{-p}{2} + \sqrt{\frac{p^2}{4} - q}}, \quad k = k_2 = \sqrt{\frac{-p}{2} - \sqrt{\frac{p^2}{4} - q}}$$

$$k = k_3 = -\sqrt{\frac{-p}{2} + \sqrt{\frac{p^2}{4} - q}}, \quad k = k_4 = -\sqrt{\frac{-p}{2} - \sqrt{\frac{p^2}{4} - q}}. \tag{B2}$$

Therefore, the general solution of eqn (31) is

$$\phi(\xi) = C_1 e^{k_1 \xi} + C_2 e^{k_2 \xi} + C_3 e^{k_3 \xi} + C_4 e^{k_4 \xi} \tag{B3}$$

where C_1, C_2, C_3 and C_4 are unknown constants to be determined from the boundary conditions. Since k_1, k_2, k_3 and k_4 may be complex numbers, it is necessary to change the form of eqn (B3) so that the general solution is expressed in terms of real numbers for various values of p and q determined from the material and geometry properties of the laminate. The parameter q is larger than zero based on its definition in eqn (5).

(I) $(p^2/4) - q < 0$.

In this case, k_1, k_2, k_3 and k_4 can be written in terms of two real numbers, α and β

$$k_1 = \sqrt{\frac{-p}{2} + \sqrt{\frac{p^2}{4} - q}} = \alpha + \beta i, \quad k_2 = \sqrt{\frac{-p}{2} - \sqrt{\frac{p^2}{4} - q}} = \alpha - \beta i$$

$$k_3 = -\sqrt{\frac{-p}{2} + \sqrt{\frac{p^2}{4} - q}} = -\alpha - \beta i, \quad k_4 = -\sqrt{\frac{-p}{2} - \sqrt{\frac{p^2}{4} - q}} = -\alpha + \beta i \tag{B4}$$

where

$$\alpha = \frac{\sqrt{-p + 2\sqrt{q}}}{2} \quad \text{and} \quad \beta = \frac{\sqrt{p + 2\sqrt{q}}}{2}. \tag{B5}$$

The general solution of eqn (31) is then expressed as

$$\phi(\beta) = C_1 \sinh[\alpha\xi] \sin[\beta\xi] + C_2 \cosh[\alpha\xi] \cos[\beta\xi] + C_3 \sinh[\alpha\xi] \cos[\beta\xi] + C_4 \cosh[\alpha\xi] \sin[\beta\xi]. \tag{B6}$$

Two particular solutions satisfying the homogeneous boundary condition at $\xi = -\rho$, i.e.,

$$\phi(\xi)|_{\xi = -\rho} = 0, \quad \left.\frac{d\phi(\xi)}{d\xi}\right|_{\xi = -\rho} = 0,$$

are constructed from eqn (B6) as

$$\phi(\xi) = u_1(\xi) = \sinh[\alpha(\xi + \rho)] \sin[\beta(\xi + \rho)]$$

$$\phi(\xi) = u_2(\xi) = \cosh[\alpha(\xi + \rho)] \sin[\beta(\xi + \rho)] - \frac{\beta}{\alpha} \sinh[\alpha(\xi + \rho)] \cos[\beta(\xi + \rho)]. \tag{B7}$$

Similarly, two particular solutions satisfying homogeneous boundary conditions at $\xi = \rho$, i.e.,

$$\phi(\xi)|_{\xi=\rho} = 0, \quad \left.\frac{d\phi(\xi)}{d\xi}\right|_{\xi=\rho} = 0,$$

are

$$\phi(\xi) = u_3(\xi) = \sinh[\alpha(\xi-\rho)]\sin[\beta(\xi-\rho)]$$

$$\phi(\xi) = u_4(\xi) = \cosh[\alpha(\xi-\rho)]\sin[\beta(\xi-\rho)] - \frac{\beta}{\alpha}\sinh[\alpha(\xi-\rho)]\cos[\beta(\xi-\rho)]. \tag{B8}$$

The functions shown in eqns (B7) and (B8) are used in eqn (33) to construct the Green's function of the problem.

The function $\phi_0(\xi)$ used in eqns (39) and (41) which satisfies eqn (31) and boundary conditions (14) is determined from the general solution, eqn (B6), as

$$\phi_0(\xi) = \frac{2(\beta\sinh[\alpha\rho]\cos[\beta\rho] + \alpha\cosh[\alpha\rho]\sin[\beta\rho])}{\beta\sinh[2\alpha\rho] + \alpha\sin[2\beta\rho]}\cosh[\alpha\xi]\cos[\beta\xi]$$
$$+ \frac{2(\beta\cosh[\alpha\rho]\sin[\beta\rho] - \alpha\sinh[\alpha\rho]\cos[\beta\rho])}{\beta\sinh[2\alpha\rho] + \alpha\sin[2\beta\rho]}\sinh[\alpha\xi]\sin[\beta\xi]. \tag{B9}$$

Equation (B9) is identical to that by Hashin (1985). It should be pointed out that the expressions of α and β used here (eqn (B5)) is more general which also applies to the case when p is larger than zero. When p is less than zero, eqn (B5) is equivalent to the expressions of α and β given by Hashin (1985).

(II) $(p^2/4) - q > 0$.

(II.1) $(p^2/4) - q > 0$ and $p > 0$.

Since q is positive, both

$$\frac{-p}{2} + \sqrt{\frac{p^2}{4} - q} \quad \text{and} \quad \frac{-p}{2} - \sqrt{\frac{p^2}{4} - q}$$

are negative in this case. Therefore, the roots k_1, k_2, k_3 and k_4 can be written as

$$k_1 = \sqrt{\frac{-p}{2} + \sqrt{\frac{p^2}{4} - q}} = \alpha i, \quad k_2 = \sqrt{\frac{-p}{2} - \sqrt{\frac{p^2}{4} - q}} = \beta i$$

$$k_3 = -\sqrt{\frac{-p}{2} + \sqrt{\frac{p^2}{4} - q}} = -\alpha i, \quad k_4 = -\sqrt{\frac{-p}{2} - \sqrt{\frac{p^2}{4} - q}} = -\beta i \tag{B10}$$

where

$$\alpha = \sqrt{\frac{p}{2} - \sqrt{\frac{p^2}{4} - q}} \quad \text{and} \quad \beta = \sqrt{\frac{p}{2} + \sqrt{\frac{p^2}{4} - q}}. \tag{B11}$$

The general solution of eqn (31) is then expressed as

$$\phi(\xi) = C_1\sin[\alpha\xi] + C_2\cos[\alpha\xi] + C_3\cos[\beta\xi] + C_4\sin[\beta\xi]. \tag{B12}$$

The functions, $u_1(\xi)$, $u_2(\xi)$, $u_3(\xi)$ and $u_4(\xi)$ used in eqn (33) are

$$\phi(\xi) = u_1(\xi) = \sin[\alpha(\xi+\rho)] - \frac{\alpha}{\beta}\sin[\beta(\xi+\rho)]$$

$$\phi(\xi) = u_2(\xi) = \cos[\alpha(\xi+\rho)] - \cos[\beta(\xi+\rho)]$$

$$\phi(\xi) = u_3(\xi) = \sin[\alpha(\xi-\rho)] - \frac{\alpha}{\beta}\sin[\beta(\xi-\rho)]$$

$$\phi(\xi) = u_4(\xi) = \cos[\alpha(\xi-\rho)] - \cos[\beta(\xi-\rho)]. \tag{B13}$$

The function $\phi_0(\xi)$ used in eqns (39) and (41) which satisfies eqn (31) and boundary conditions (14) is determined from the general solution, eqn (B12), as

$$\phi_0(\xi) = \frac{\alpha\sin[\alpha\rho]\cos[\beta\xi] - \beta\sin[\beta\rho]\cos[\alpha\xi]}{\alpha\sin[\alpha\rho]\cos[\beta\rho] - \beta\sin[\beta\rho]\cos[\alpha\rho]}. \tag{B14}$$

(II.2) $(p^2/4) - q > 0$ and $p < 0$.

Both

$$\frac{-p}{2}+\sqrt{\frac{p^2}{4}-q} \quad \text{and} \quad \frac{-p}{2}-\sqrt{\frac{p^2}{4}-q}$$

are positive in this case. The roots k_1, k_2, k_3 and k_4 can be written as

$$k_1=\sqrt{\frac{-p}{2}+\sqrt{\frac{p^2}{4}-q}}=\alpha, \quad k_2=\sqrt{\frac{-p}{2}-\sqrt{\frac{p^2}{4}-q}}=\beta$$
$$k_3=-\sqrt{\frac{-p}{2}+\sqrt{\frac{p^2}{4}-q}}=-\alpha, \quad k_4=-\sqrt{\frac{-p}{2}-\sqrt{\frac{p^2}{4}-q}}=-\beta \tag{B15}$$

where

$$\alpha=\sqrt{\frac{-p}{2}+\sqrt{\frac{p^2}{4}-q}} \quad \text{and} \quad \beta=\sqrt{\frac{-p}{2}+\sqrt{\frac{p^2}{4}-q}}. \tag{B16}$$

The general solution of eqn (31) is then expressed as

$$\phi(\xi)=C_1\sinh[\alpha\xi]+C_2\cosh[\alpha\xi]+C_3\cosh[\beta\xi]+C_4\sinh[\beta\xi]. \tag{B17}$$

The functions, $u_1(\xi)$, $u_2(\xi)$, $u_3(\xi)$ and $u_4(\xi)$ are

$$\phi(\xi)=u_1(\xi)=\sinh[\alpha(\varepsilon+\rho)]-\frac{\alpha}{\beta}\sinh[\beta(\xi+\rho)]$$
$$\phi(\xi)=u_2(\xi)=\cosh[\alpha(\xi+\rho)]-\cosh[\beta(\xi+\rho)]$$
$$\phi(\xi)=u_3(\xi)=\sinh[\alpha(\xi-\rho)]-\frac{\alpha}{\beta}\sinh[\beta(\xi-\rho)]$$
$$\phi(\xi)=u_4(\xi)=\cosh[\alpha(\xi-\rho)]-\cosh[\beta(\xi-\rho)]. \tag{B18}$$

The function $\phi_0(\xi)$ used in eqns (39) and (41) which satisfies eqn (31) and boundary conditions (14) are determined from the general solution, eqn (B18), as

$$\phi_0(\xi)=\frac{\alpha\sinh[\alpha\rho]\cosh[\beta\xi]-\beta\sinh[\beta\rho]\cosh[\alpha\xi]}{\alpha\sinh[\alpha\rho]\cosh[\beta\rho]-\beta\sinh[\beta\rho]\cosh[\alpha\rho]}. \tag{B19}$$

(III) $(p^2/4)-q=0$.

(III.1) $(p^2/4)-q=0$, $p<0$.

The roots k_1, k_2, k_3 and k_4 can be written as

$$k_1=k_2=\sqrt{\frac{-p}{2}}=\alpha, \quad k_3=k_4=-\sqrt{\frac{-p}{2}}=-\alpha. \tag{B20}$$

The general solution of eqn (31) is then expressed as

$$\phi(\xi)=C_1\sinh[\alpha\xi]+C_2\cosh[\alpha\xi]+C_3\xi\cosh[\alpha\xi]+C_4\xi\sinh[\alpha\xi]. \tag{B21}$$

The functions, $u_1(\xi)$, $u_2(\xi)$, $u_3(\xi)$ and $u_4(\xi)$ are

$$\phi(\xi)=u_1(\xi)=(\xi+\rho)\sinh[\alpha(\xi+\rho)]$$
$$\phi(\xi)=u_2(\xi)=\sinh[\alpha(\xi+\rho)]-\alpha(\xi+\rho)\cosh[\alpha(\xi+\rho)]$$
$$\phi(\xi)=u_3(\xi)=(\xi-\rho)\sinh[\alpha(\xi-\rho)]$$
$$\phi(\xi)=u_4(\xi)=\sinh[\alpha(\xi-\rho)]-\alpha(\xi-\rho)\cosh[\alpha(\xi-\rho)]. \tag{B22}$$

The functions $\phi_0(\xi)$ used in eqns (39) and (41) which satisfies eqn (31) and boundary conditions (14) is determined from the general solution, eqn (B21) as

$$\phi_0(\xi)=2\frac{\alpha\rho\cosh[\alpha\rho]+\sinh[\alpha\rho]}{2\alpha\rho+\sinh[2\alpha\rho]}\cosh[\alpha\xi]-2\frac{\alpha\sinh[\alpha\rho]}{2\alpha\rho+\sinh[2\alpha\rho]}\xi\sinh[\alpha\xi]. \tag{B23}$$

(III.2) $(p^2/4)-q=0$, $p>0$.

The roots k_1, k_2, k_3 and k_4 can be written as

$$k_1 = k_2 = \sqrt{\frac{-p}{2}} = \alpha i, \quad k_3 = k_4 = -\sqrt{\frac{-p}{2}} = -\alpha i. \tag{B24}$$

The general solution of eqn (31) is then expressed as

$$\phi(\xi) = C_1 \sin[\alpha\xi] + C_2 \cos[\alpha\xi] + C_3 \xi \cos[\alpha\xi] + C_4 \xi \sin[\alpha\xi]. \tag{B25}$$

The functions, $u_1(\xi)$, $u_2(\xi)$, $u_3(\xi)$ and $u_4(\xi)$ are

$$\begin{aligned}
\phi(\xi) &= u_1(\xi) = (\xi+\rho)\sin[\alpha(\xi+\rho)] \\
\phi(\xi) &= u_2(\xi) = \sin[\alpha(\xi+\rho)] - \alpha(\xi+\rho)\cos[\alpha(\xi+\rho)] \\
\phi(\xi) &= u_3(\xi) = (\xi-\rho)\sin[\alpha(\xi-\rho)] \\
\phi(\xi) &= u_4(\xi) = \sin[\alpha(\xi-\rho)] - \alpha(\xi-\rho)\cos[\alpha(\xi-\rho)].
\end{aligned} \tag{B26}$$

The function $\phi_0(\xi)$ used in eqns (39) and (41) which satisfies eqn (31) and boundary conditions (14) is determined from the general solution, eqn (B25), as

$$\phi_0(\xi) = 2\frac{\alpha\rho\cos[\alpha\rho] + \sin[\alpha\rho]}{2\alpha\rho + \sin[2\alpha\rho]}\cos[\alpha\xi] + 2\frac{\alpha\sin[\alpha\rho]}{2\alpha\rho + \sin[2\alpha\rho]}\xi\sin[\alpha\xi]. \tag{B27}$$